A Novel Multimodal Cognitive Interaction for Walker-Assisted Rehabilitation Therapies

Wandercleyson M. Scheidegger[1], Ricardo C. de Mello[1], Sergio D. Sierra M.[2], Mario F. Jimenez[3], Marcela C. Múnera[2], Carlos A. Cifuentes[2] and Anselmo Frizera-Neto[1], *Member, IEEE*

***Abstract*— This work presents a multimodal cognitive interaction strategy aiming at walker-assisted rehabilitation therapies, with special focus on post-stroke patients. Such interaction strategy is based on monitoring user's gait and face orientation to command the displacement of the smart walker. Users are able to actively command the steering of the walker by changing their face orientation, while their lower limbs movement affect the walker's linear velocity. The proposed system is validated using a smart walker and the results obtained point to the feasibility of employing such cognitive interaction in rehabilitation therapies.**

I. INTRODUCTION

Totaling 982 million people in 2017, the overall elderly population is expected to double by 2050, reaching 2.1 billion people over 60 years old [1]. Sensory-motor, cognitive, and mobility impairments are often associated with aging [2] and the current demographic prospects demand efforts from public and private actors to attend to the specific needs of the elderly.

Individuals debilitated by chronic diseases, walking disabilities or age-related problems need to overcome a number of challenges to continue living independently or in a way that improves their quality of life [2]. Thus, it is necessary to improve on their ability to perform daily activities, such as the simple action of walking without the help of another person or going from one environment to another in their residence [2]. Assistive devices such as wheelchairs, walking sticks, walkers, and crutches may be used to assist people with motor difficulties to move more autonomously [3]. However, depending on the level of the impairment, the use of such devices may not be enough for assuring a reasonable level of independence.

The introduction of robotics concepts into assistive devices allowed researchers to invest in more effective ways to assess patient state and to assist in rehabilitation [3]. For instance, smart walkers integrate electronics, sensors, and actuators over conventional walkers to provide and improve functionality such as physical support, sensorial assistance, cognitive assistance, and health monitoring. Smart walkers can also leverage multimodal interfaces to interact with the user and to detect human motion intentions with high precision [4].

[1] Graduate Program on Electrical Engineering, Federal University of Espírito Santo, Vitória, Brazil

2 Department of Biomedical Engineering, Colombian School of Engineering Julio Garavito, Bogotá D.C., Colombia

3 Department of Bioengineering Graduate Program, El Bosque University, Bogotá D.C., Colombia

Most multimodal interaction strategies designed for smart walkers leverage several modes of physical interaction between user and walker [5]. Usually, the physical interaction is measured by force sensors and such data is used to infer the user's motion intentions and feed the walker's controller to command its displacement [6]. Admittance-based controllers (e.g., [4], [5], [7]) are commonly implemented in the literature under the assumption of the user being able to exert upper limbs force patterns compatible with their own movement intentions.

Thus, such class of interaction strategy renders itself unsuitable when the user presents unbalanced or inconsistent interaction/supporting forces, which deeply degrades the quality of the detection of motion intentions through physical interfaces. For instance, the most common motor deficit after stroke is paresis of the side of the body contralateral to the cerebrovascular event, which may weaken and even inhibit upper limb movements [8]. Conventional walkers have been used in the rehabilitation of post-stroke patients [9], but there is still a lack of studies using smart walkers in such kind of treatment. As smart walkers can augment the capabilities of regular walkers in therapy [10], there is a need for developing interaction strategies capable of attending to user commands despite possible unbalance in interaction forces.

The use of multimodal cognitive interfaces can overcome the limitations imposed by pure physical interfaces. Such class of interfaces allow the collection of data regarding the user through audio, visual, and/or active ranging sensing [4]. Ultimately, interaction strategies based on cognitive interfaces can be fused with strategies based on physical interaction to generate robust interfaces capable of attending to users presenting a wide range of impairments (e.g., [7]).

Cognitive interaction strategies have been presented focusing on patients with cerebral palsy [11] and post-stroke patients [12], both leveraging laser range finders (LRF) sensors to monitor user gait and control the distance between user and walker. In Cifuentes *et al.* [11], the user physically controls the steering of the walker through a handlebar, while that in Loterio *et al.* [12], the user was only asked to walk in a straight line. Valadão *et al.* [13] later expanded the interaction strategy presented in [12] to infer user's turning intentions, though such strategy was validated only using healthy subjects. In a later work, Cifuentes *et al.* [4] also presented a follow-in-front strategy for a smart walker leveraging multimodal cognitive interfaces to accomplish the following.

This work presents a multimodal cognitive interaction

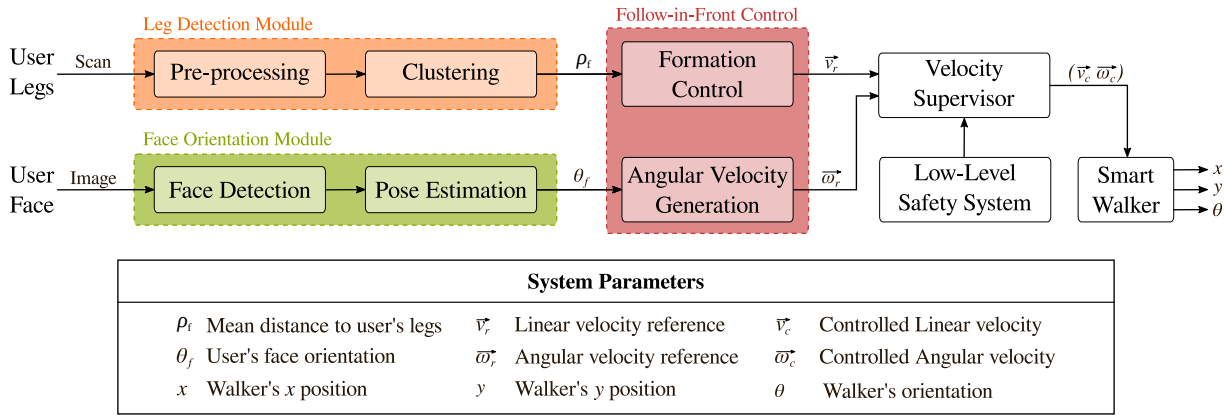

Fig. 1. Block diagram of our multimodal cognitive interaction.

strategy aiming at walker-assisted rehabilitation therapies, with special focus on post-stroke patients. Such interaction strategy is based on monitoring user's gait and face orientation to command the displacement of the smart walker. In such a follow-in-front strategy, the users are able to actively command the steering of the walker by changing their face orientation, while their lower limbs movement affects the walker's linear velocity.

Over the next sections, we describe the overall strategy and controllers focusing on a smart walker implementation, and validate the system without physical contact between user and walker. The final goal of this work is to integrate such multimodal interaction strategy to controllers based on physical interaction for clinical use.

II. MULTIMODAL INTERACTION STRATEGY

Previous works from our group have evidenced the limitations of multimodal interaction strategies in which the movement of a smart walker is mainly controlled by physical interfaces. In particular, hemiparetic post-stroke patients can not adequately cope with some of such interaction strategies due to partial limb weakness. In this section, we present a novel multimodal interaction strategy focusing on future implementation for post-stroke rehabilitation therapies.

We propose a cognitive interaction strategy based on two communication channels: a visual channel, leveraging video acquired by a camera pointing towards the face of the user; and an active ranging channel, based on data measured by an LRF sensor directed towards user's lower limbs. Figure 1 brings the block diagram illustrating each module of our interaction strategy and their interconnections. Figure 2(a) illustrates our multimodal cognitive interaction channels integrated into a smart walker. Data gathered by those two interfaces is processed to feed our follow-in-front control strategy, the main building block of the interaction strategy proposed in this work.

A. Leg Detection Module

A LRF sensor is used for leg detection and leg distance estimation (see Fig. 1). To constrain the sensor's filed of

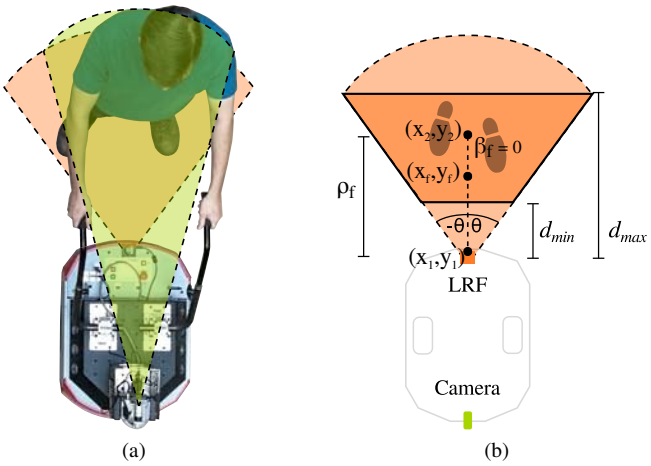

Fig. 2. Multimodal cognitive interaction channels: a) user-walker top view illustrating the visual and active ranging sensing channels; b) conceptual view of the walker illustrating the lower limbs detection zone and the formation variables of the *Follow-in-Front Control* module.

view, a polygon is defined based on distance thresholds, d_{min}, d_{max}, and a desired opening angle, θ, (see Fig. 2(b)). The *pre-processing* sub-module receives the data from the LRF sensor and considers the points inside the reference polygon. Such selection is aimed at discarding the data points outside of the polygon, and thus minimizing the detection of undesired nearby objects (e.g. passing people). Additionally, the laser readings feed a classifier based on unsupervised learning, which groups the laser points and classifies such points as either user legs or noise. Then, the *clustering* sub-module separates the information regarding each leg using the DBSCAN technique (i.e. Density-Based Spatial Clustering of Applications with noise) [14]. The algorithm requires two parameters to be set: (1) the minimum distance to group two points; and (2) the minimum number of grouped points to define a cluster. The user position and distance, ρ_f, in relation to the robot, is then defined using the center of each cluster and the mean distance between them (see Fig. 3).

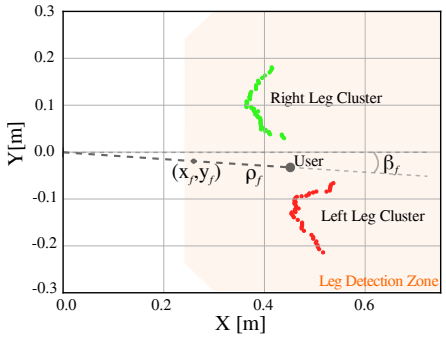

Fig. 3. Laser scan plot illustrating the *Leg Detection* module: the points within the leg detection zone are clusterized for leg identification and distance extraction.

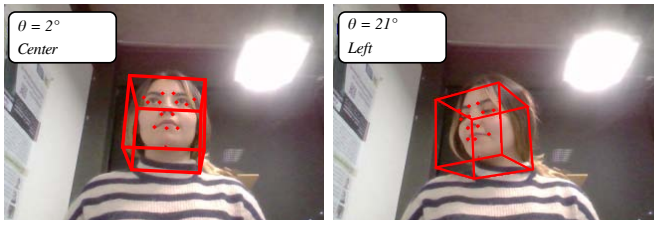

(a) (b)

Fig. 4. Collection of images illustrating the *Face orientation* module: a) user is facing forward and the estimated pose shows a 2° horizontal angle, thus classifying as a "center" orientation; b) user turns face to the left and pose estimation changes accordingly.

B. Face Orientation Module

This module uses a video stream captured by the camera to estimate the orientation of the user's face with respect to the walker. The images captured from the camera are processed in the *Face Detection* module using the Dlib python library [15]. Dlib uses machine learning concepts to detect faces in the image and find standard landmarks on them (see Fig. 4). The *Pose Estimation* module uses these landmarks to estimate the horizontal angle θ_f between the normal vector of the user's face plane and the walker. It also prevents discontinuities in the movement caused by errors in the detection of the user's face. When maneuvering, the user might turn the face to an extreme, making it impossible for the algorithm to detect it. The algorithm discards small discontinuities to avoid classification errors or sudden movements of the head, which can degrade control quality.

C. Follow-in-Front Control

The outputs of the *Leg Detection* and *Face Orientation* modules feed the *Follow-in-Front Control* module, which is responsible for generating the walker's reference linear and angular velocities, v_r and ω_r, respectively. The *Formation Control* sub-module generates the reference linear velocity v_r according to a multi-layer control strategy for a leader-follower formation. The objective is to ensure that the robot will follow in front of the person, the leader of the formation, by maintaining the distance ρ_f close to a desired distance value. Such module is based on the controller proposed by Brandão *et al.* [16]. The formation is described by:

$$\mathbf{q_f} = \begin{bmatrix} x_f & y_f \\ \beta_f & \rho_f \end{bmatrix} \tag{1}$$

where x_f, y_f define the formation pose (see Fig. 2(b) and Fig. 3) and β_f, ρ_f define the formation shape (see Fig. 3). The controller defines a desired formation pose and shape $\mathbf{q}_{\text{des}}$ and its derivative, $\dot{\mathbf{q}}_{\text{des}}$, given the position of the user and walker [16], and the formation error is defined by $\tilde{\mathbf{q}} = \mathbf{q}_{\text{des}} - \mathbf{q}_{\text{f}}$. With the time derivative of the forward and the inverse kinematics transformations for the smart walker, the proposed formation control law is:

$$v_r = \mathbf{K_r} J^{-1}(\dot{\mathbf{q}}_{\text{des}} + \mathbf{L}\tanh(\mathbf{L^{-1}}\kappa\tilde{\mathbf{q}})) \tag{2}$$

where $\mathbf{K_r}$ is the forward kinematics of the smart walker, J^{-1} is its Jacobian inverse matrix, and κ and $\mathbf{L}$ are positives definite diagonal gain matrices.

The Angular Velocity Generation block generates the reference angular velocity ω_r. The block receives the θ_f from the Pose Estimation block and according to how long the user's face remains in position, the angular velocity increases exponentially. This strategy avoids abrupt changes on the angular velocity and ensures that the greater permanence in a certain orientation expresses a stronger intention to perform the movement in the required direction. The proposed equation for angular velocity is

$$\omega_r = \alpha\left(1 + \tanh\left(\frac{\beta t_{\theta_d}}{\gamma}\right)\right) sign(\theta_d) \tag{3}$$

where α, β, and γ are tunning paramters, t_{θ_d} is the time that user's face remained in current position, and θ_d is a discrete value which is positive if the user's is facing the left, negative if right, and zero otherwise.

D. Velocity Supervisor and Safety System

The *Low-Level Safety System* monitors other sensors, such as a second LRF or sonars, to detect nearby obstacles. If an obstacle is detected near the smart walker, the *Low-Level Safety System* sends a flag to the *Velocity Supervisor*, which is responsible for stopping the walker. Moreover, the *Velocity Supervisor* monitors the output of the *Follow-in-Front Control* to avoid errors and to saturate possible abnormally high values.

III. EXPERIMENTAL PROTOCOL

A. Materials

To validate the Multimodal Interaction Strategy previously described, the equipments presented in the following sections were used.

1) AGoRA Smart Walker: all the blocks displayed in Figure 1 are implemented on the smart walker presented in Sierra *et al.* [17]. Since the proposed multimodal strategy does not require any physical contact between the user and the walker, the handlebars and force sensors are disposed. The *AGoRA Smart Walker* is mounted on a robotic platform

with an on-board PC running a Linux operating system distribution and the Robotic Operating System (ROS) framework. The platform is equipped with:

- 2 Motorized wheels and two caster wheels for robot's propulsion and stability.
- 2 Encoders and an Inertial Measurement Unit (IMU) to measure robot's ego-motion.
- 1 Light Detection and Ranging Sensor (LiDAR) (S300 Expert, SICK, Germany) and 2 ultrasonic boards for obstacles detection and low-level safety system implementation.

2) HD Camera: An HD camera (LifeCam Studio, Microsoft, U.S.A) is attached to the *Pioneer LX*'s deck point to the face of the user to capture video.

3) Laser Range-Finder (LRF): An LRF (Hokuyo URG-04LX-UG01, Japan) is used to monitor user's lower limbs.

4) External CPU: An external computer is used for execution of processing tasks, being responsible for hosting the computation of most of the system's modules. Only critical systems (i.e., sensor acquisition, low-level actuation, safety and supervisor modules) were processed in the smart walker's on-board computer. The communication with the external CPU was be achieved through the *Pioneer LX*'s Wi-Fi modules using ROS network communication protocols.

B. Participants Recruitment

Five volunteers were formally recruited to participate in the validation tests. As this work focus on validating the proposed multimodal interaction strategy, the inclusion criteria were as follows: (a) Healthy volunteers, (b) volunteer height ranging from $1.7\ m$ to $1.85\ m$, and (c) age over 18 years. Likewise, the exclusion criteria were: (a) volunteers with cognitive disability, (b) lower limbs impairments or volunteers with physical disability, (c) volunteers with visual impairment, and (d) age over 60 years.

C. Session Environment and Procedure

The validation trials took place at the lobby of the laboratory building of the Colombian School of Engineering. To test different lighting conditions that could impact the quality of the imaging processing modules, the trials were performed early in the morning, at noon and at sunset.

Every session consisted in three different trials of specific path following tasks. Each participant was asked to follow three paths marked on the floor. The first path was formed by a $10m$ straight line, and it was aimed at assessing the formation control performance. In such trial, the HD camera was removed from the walker and only the *Leg Detection* module was used. The second path was formed by a Lemniscate of Bernoulli defined by a parameter $a = 2.5m$, and it was intended to evaluate the behaviour of the complete follow-in-front control (i.e., both *Leg Detection* and *Face Orientation* modules simultaneously working). Finally, the third trial was constituted by an square-shaped path ($3m$ sides), including an obstacle in one of its segments. The third path, seek to assess the controller response at an obstacle avoidance task.

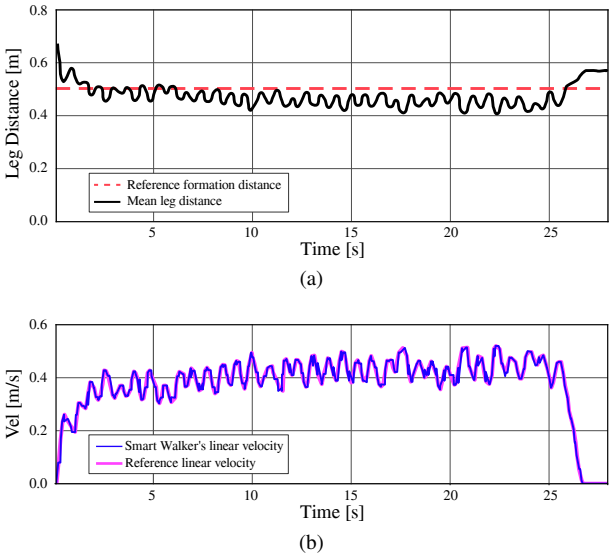

Fig. 5. Results obtained from the straight line trials: a) measured leg distance and desired formation distance; b) acquired linear velocities.

At the beginning of the session, the volunteer was instructed in the behaviour of the follow-in-front controller. Before the accomplishment of each trial, the participants were allowed to interact with the platform, in order to allow them to understand its behaviour. During trials, the researchers stayed out of the session environment to avoid interfering. At the end of each trial, a data log including controller and walker's information was stored. Likewise, at each trial, a video was recorded for further analysis purposes.

IV. RESULTS AND DISCUSSION

The five subjects completed the trials without difficulties and managed to interact with the smart walker to follow the indicated paths. Regarding the straight line trials, subjects presented a mean gait speed of $0.41 \pm 0.05m/s$, which is compatible with gait speeds observed in the smart walker literature (e.g., inferior to $0.6m/s$ [18] or to $0.4m/s$ [7]). Figure 5 displays formation and velocity data observed during the participation of subject 1, which presented a mean gait speed of $0.46m/s$ during the experiment. The way the formation variable (i.e., distance between user and walker) changes in time is shown in Fig. 5(a). As the subject increases pace after the first ten seconds, the formation variable decreases, leading to an increase in the corresponding linear velocity observed in Fig. 5(b). The oscillatory nature of the measured velocities are a direct result of the human gait, as the formation variable decreases to a minimum peak at every heel strike. The controller parameters can be set to prioritize minimizing the formation error (i.e., by increasing gains) or to prioritize slower, and possibly safer, gait speeds, depending on the user condition. As the smart walker moves, the controller closes the cognitive loop by indicating to the user an adequate pace.

During the leminiscate and square trials, subjects presented a mean gait speed of $0.29 \pm 0.06m/s$ and $0.29 \pm$

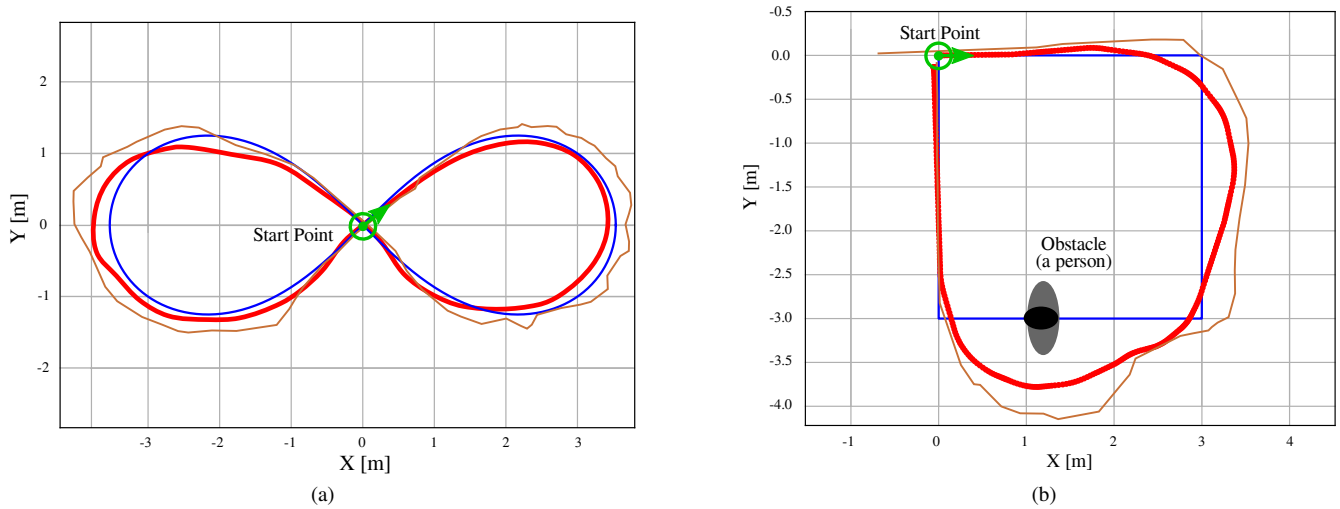

Fig. 6. Results from leminiscate and square trials, the blue line represents the ideal path, the red line is the robot's odometry, and the brown line represents the user position as gathered by the LRF: a) subject is able to follow the leminiscate path without large deviations; b) subject deviates from the path due to its sharp curves and obstacle.

$0.07m/s$, respectively. The velocities were lower than in the ones observed in the straight line trials due to low maneuverability [6] of the AGoRA walker, in which the center of rotation is far from the user. Nevertheless, such velocities are compatible with the literature and gait speed is likely to increase in smart walkers with higher maneuverability, such as the one presented by Jimenez *et al.* [7].

Figure 6 brings the odometry plots of the leminiscate and square trials performed by subject 1. It can be seen in Fig. 6(a) that the user was able to follow the desired path adequately without large deviations. The square trial imposed more difficulty to the following due to its sharp curves. Figure 6(b) portraits a typical result: the user starts steering the walker before the first curve but can not get back to the path fast enough while trying to maintain pace. By the time the user brings the walker back to the path, the next curve is close and there is an obstacle ahead. The area around the point $(2.2, -3.4)$ in Fig. 6(b) represents the moment in which the subject stopped attempting to return to the path and started focusing on deviating from the obstacle. Such deviation results on a soft approach to the last curve and a better path following during the ending of the trial. Again, the low maneuverability of the AGoRA walker plays a role in the results, and it can be seen in Fig. 6 the discrepancies between the path performed by the user (brown line) and by the robot (red line).

Figure 7 displays the velocities observed during the leminiscate trial performed by subject 1 (i.e., same trial as portrait by Fig. 6(a)). Despite the overall decrease of mean gait speed in the leminiscate trials when compared with the straight line trials, it can be seen that the gait speed is somewhat uniform throughout the trial and no significant reduction is observed when steering the walker. Figure 7 also highlights the behaviour of the *Angular Velocity Generation* module

Table I shows the accuracy observed in the *Face Detection*

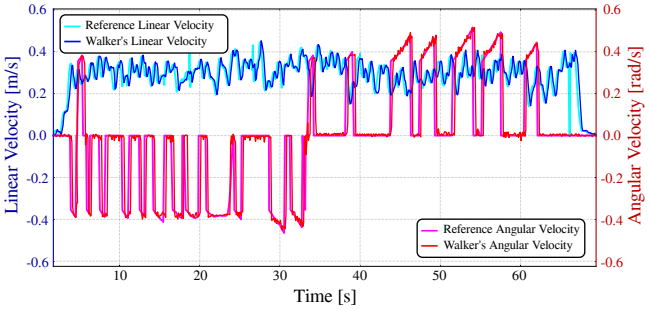

Fig. 7. Leminiscate trial results: behavior of the *Follow-in-Front Control* module.

module. The best accuracy values were observed during the lemniscate trials. In fact, due to its soft curves, such path demands less abrupt variations on the face's horizontal orientation when compared to the square-shaped path. During the square trials, the subjects tended to increase their faces' horizontal orientation to overcome the sharp curves. This behavior hampers the quality of the face detection algorithm. The relevant distict characteristics of each subject are also shown in Table I, which also played a role in affecting the face detection accuracy. Nevertheless, even under low accuracy results, all the subjects could interact with the walker and successfully complete the trials.

The average control loop frequency observed throughout the trials was $8.95Hz$, value that slightly grows to $9.29Hz$ if we consider only the data from the straight line trials. Despite bounded by the LRF's $10Hz$ working frequency, the control loop frequency does not suffer much from the added CPU overhead due to the *Face Orientation* module processing. This also plays a role in the fact that the proposed interaction strategy works even when the face detection accuracy is low, as observed in the square trials with subjects 4 and 5 (see Table I): as the mean rate of processed video frames was $26.6Hz$, the *Face Orientation* module provides at least two

TABLE I

LEMINISCATE AND SQUARE TRIALS RESULTS: ACCURACY OF THE FACE DETECTION SUB-MODULE.

Subject	Gender	Path	Face Detection Accuracy	Distinct Characteristics
1	Male	Leminiscate Square	91.35 % 95.74 %	No Facial Hair
2	Male	Leminiscate Square	90.54 % 81.38 %	No Facial Hair
3	Male	Leminiscate Square	95.22 % 86.79 %	Goatee
4	Female	Leminiscate Square	78.84 % 59.37 %	Long Hair
5	Male	Leminiscate Square	73.66 % 52.56 %	Beard

samples of information to the *Follow-in-Front Control* per laser scan.

V. CONCLUSIONS AND FUTURE WORK

This work presented a novel multimodal cognitive interaction for walker-assisted rehabilitation therapies. The development of such interaction strategy focuses on users that present unbalanced or inconsistent interaction/supporting forces patterns, a class of impairment that is commonly observed in post-stroke patients. Our cognitive interaction strategy is based on monitoring user's gait and face orientation to command the displacement of the smart walker. We validated the proposed system using a smart walker and the results obtained point to the feasibility of using such interaction strategy.

We believe that the multimodal interaction presented in this work is suitable for walker-assisted rehabilitation therapies on post-stroke patients with upper limbs movement limitations. Nevertheless, there is still a need for implementing and testing our system in different types of smart walkers to evaluate ideal conditions of weight bearing and maneuverability before starting with clinical trials. As an important future work, we believe that it is fundamental to merge our cognitive system with physical interaction strategies. In particular, by fusing the output of our *Follow-in-Front Control* module to an admittance-based controller, such as the one presented in Jimenez *et al.* [7], we might achieve softer velocity outputs. This should ultimately increase the safety of our system while also increasing the target population of users. We also intend to implement a new machine learning algorithm that is currently under development by our group to improve the face detection system and to leverage the cloud robotics paradigm by integrating our system to a cloud computing platform, which seems to be a promising technology for smart walkers [19].

ACKNOWLEDGMENT

The research leading to these results received funding from the European Commission H2020 program under grant agreement no. 688941 (FUTEBOL), as well from the Brazilian MCTIC through RNP and CTIC. This work was partially supported by FAPES (80709036 & 72982608), and CNPq (304192/2016-3). This study was financed in part by the Coordenação de Aperfeiçoamento de Pessoal de Nivel Superior – Brasil (CAPES) - Finance Code 001. This work was supported by Colombia Colciencias (Grant 801-2017) and Colombian School of Engineering Julio Garavito Funds.

REFERENCES

[1] United Nations, "World Population Ageing 2017," *World Population Ageing 2017*, pp. 1–124, 2017.

[2] K. Doughty and G. Williams, "New models of assessment and prescription of smart assisted living technologies for personalised support of older and disabled people," *Journal of Assistive Technologies*, vol. 10, no. 1, pp. 39–50, 2016.

[3] M. Martins, C. Santos, A. Frizera, and R. Ceres, "A review of the functionalities of smart walkers," *Medical Engineering & Physics*, vol. 37, no. 10, pp. 917 – 928, 2015.

[4] C. A. Cifuentes and A. Frizera, "Human-robot interaction for assisting human locomotion," in *Springer Tracts in Advanced Robotics*, 2016, vol. 115, pp. 17–31.

[5] J. Paulo, P. Peixoto, and U. J. Nunes, "Isr-aiwalker: Robotic walker for intuitive and safe mobility assistance and gait analysis," *IEEE Transactions on Human-Machine Systems*, vol. 47, no. 6, pp. 1110–1122, Dec 2017.

[6] S. Page, L. Saint-Bauzel, P. Rumeau, and V. Pasqui, "Smart walkers: an application-oriented review," *Robotica*, vol. 35, no. 6, p. 12431262, 2017.

[7] M. F. Jiménez, M. Monllor, A. Frizera, T. Bastos, F. Roberti, and R. Carelli, "Admittance controller with spatial modulation for assisted locomotion using a smart walker," *Journal of Intelligent & Robotic Systems*, May 2018.

[8] F. de N. A. P. Shelton and M. J. Reding, "Effect of lesion location on upper limb motor recovery after stroke," *Stroke*, vol. 32, no. 1, pp. 107–112, 2001.

[9] P. Langhorne, J. Bernhardt, and G. Kwakkel, "Stroke rehabilitation," *The Lancet*, vol. 377, no. 9778, pp. 1693 – 1702, 2011.

[10] O. Postolache, J. M. Dias Pereira, V. Viegas, L. Pedro, P. S. Girao, R. Oliveira, and G. Postolache, "Smart walker solutions for physical rehabilitation," *IEEE Instrumentation Measurement Magazine*, vol. 18, no. 5, pp. 21–30, October 2015.

[11] C. A. Cifuentes, C. Bayon, S. Lerma, A. Frizera, and E. Rocon, "Human-robot interaction strategy for overground rehabilitation in patients with cerebral palsy," in *2016 6th IEEE International Conference on Biomedical Robotics and Biomechatronics*, June 2016, pp. 729–734.

[12] F. A. Loterio, C. T. Valadao, V. F. Cardoso, A. Pomer-Escher, T. F. Bastos, and A. Frizera-Neto, "Adaptation of a smart walker for stroke individuals: a study on sEMG and accelerometer signals," *Research on Biomedical Engineering*, vol. 33, pp. 293 – 300, 10 2017.

[13] C. Valado, E. Caldeira, T. Bastos-Filho, A. Frizera-Neto, and R. Carelli, "A new controller for a smart walker based on human-robot formation," *Sensors*, vol. 16, no. 7, 2016.

[14] M. Daszykowski and B. Walczak, "Density-Based Clustering Methods," *KDD-96 Proceedings*, vol. 96, no. 34, pp. 226–231, 1996.

[15] D. A. King, "Dlib-ml: A Machine Learning Toolkit," *Journal of Machine Learning Research*, vol. 10, pp. 1755–1758, 2009. [Online]. Available: http://dlib.net/

[16] A. S. Brandao, F. N. Martins, V. T. L. Rampinelli, M. Sarcinelli-Filho, T. F. Bastos-Filho, and R. Carelli, "A multi-layer control scheme for multi-robot formations with adaptive dynamic compensation," in *2009 IEEE International Conference on Mechatronics*, April 2009, pp. 1–6.

[17] S. D. Sierra, J. F. Molina, D. A. Gómez, M. C. Múnera, and C. A. Cifuentes, "Development of an interface for human-robot interaction on a robotic platform for gait assistance: Agora smart walker," in *2018 IEEE ANDESCON*, Aug 2018, pp. 1–7.

[18] C. Werner, G. P. Moustris, C. S. Tzafestas, and K. Hauer, "User-Oriented Evaluation of a Robotic Rollator That Provides Navigation Assistance in Frail Older Adults with and without Cognitive Impairment," *Gerontology*, pp. 278–290, 2017.

[19] R. C. Mello, M. F. Jimenez, M. R. N. Ribeiro, R. Laiola Guimares, and A. Frizera-Neto, "On human-in-the-loop cps in healthcare: A cloud-enabled mobility assistance service," *Robotica*, p. 117, 2019.